Contents lists available at ScienceDirect

Solid State Communications

journal homepage: www.elsevier.com/locate/ssc

On the compression behavior of Ti_2InC, $(Ti_{0.5}, Zr_{0.5})_2InC$, and M_2SnC ($M = Ti$, Nb, Hf) to quasi-hydrostatic pressures up to 50 GPa

Bouchaib Manoun [a,b,*], O.D. Leaffer [c], S. Gupta [c], E.N. Hoffman [c], S.K. Saxena [b], J.E. Spanier [c], M.W. Barsoum [c]

[a] *Laboratoire de Physico-Chimie des Matériaux, Département de Chimie, FST Errachidia, University Moulay Ismail, Morocco*
[b] *Center for Study of Matter at Extreme Conditions, Florida International University, VH-140, University Park, Miami, FL 33199, USA*
[c] *Department of Materials Science and Engineering, Drexel University, Philadelphia, PA 19104, USA*

ARTICLE INFO

ABSTRACT

Using a synchrotron X-ray radiation source and a diamond anvil cell we measured the dependences of the lattice parameters on quasi-hydrostatic pressure of the order of 50 GPa of the following MAX phases: Ti_2InC, $(Ti_{0.5}, Zr_{0.5})_2InC$, Zr_2InC and Ti_2SnC, Nb_2InC and Hf_2InC. Like other MAX phases, the phases studied herein were all stable up to ≈ 50 GPa. In both series, the substitution of Ti ($r = 1.32$ Å) by the larger sized metals, Zr or Nb (with r varying between 1.34 and 1.55 Å) resulted in larger unit cell parameters and volumes. At 152 ± 3 and 148 ± 3 GPa, the respective bulk moduli, K_o, of Ti_2SnC and Ti_2InC are quite comparable. Replacing Ti by Hf or Nb in Ti_2SnC leads to increases in K_o by 11% and 18%, respectively. Conversely, replacing half the Ti by Zr in Ti_2InC leads to a 13% drop in K_o; replacing all of the Ti drops it by 16.5%. Most of these trends are reproduced in our *ab initio* calculations of K_o. For all compositions, the compressibilities along the c-direction were greater than those along the a-direction. For the M_2SnC series, the compressibilities along the c-axes were quite similar; the compressibilities along the a-axis of Ti_2SnC were greater than in the Nb- or Hf-containing ternaries. The c-axis compressibilities of the In-containing compounds were almost indistinguishable. The compressibilities along the a-axes of $(Ti_{0.5}, Zr_{0.5})_2InC$ and Zr_2InC were also quite comparable; those of Ti_2InC was less compressible.

© 2009 Published by Elsevier Ltd

1. Introduction

The $M_{n+1}AX_n$ (MAX) compounds, where $n = 1, 2$ or 3, M is an early transition metal, A is an A-group (mostly IIIA and IVA) element, and X is C or N, have been studied extensively these last few years [1–9]. These compounds adopt a hexagonal crystal structure (space group $P6_3/mmc$), with two formula units per unit cell, consisting of layers of edge-sharing MC_6 octahedra interleaved with square-planar A layers. The octahedra are identical to those found in the rock salt structure of the corresponding binary compounds, MX [10]. The phases studied in this work belong to the $n = 2$, or 211, subgroup.

The MAX phases have been widely studied due to their commercial potential. Most are good thermal and electrical conductors, damage tolerant and thermal shock resistant. They are relatively soft (Vickers hardness ≈ 2–8 GPa) and readily machinable [11]. Some of them, most notably Ti_3SiC_2 and Ti_2AlC, are promising candidates for high-temperature structural

applications, because of their high-temperature strengths and good oxidation resistance even under severe thermal cycling [12]. Many are elastically quite stiff, with densities comparable to that of Ti metal, and Debye temperatures (700 K) that are quite high [13–15]. This combination of properties derives partially from the metallic nature of the bonding, partially from the layered nature of the structure and partially from the fact that basal plane dislocations are mobile at all temperatures. We have also recently shown that the attenuation of sound waves in Ti_2AlC was higher than that of many woods and comparable to that of some polymers [16,17].

Over the last few years a concerted effort has been made to try to understand the relationship between MAX phase chemistries and their mechanical and elastic properties. Most germane to this paper are the isothermal bulk moduli, K_o. Manoun et al. [18–25] reported the K_o values of M_2AlC ($M = $ Ti, V, Cr, Nb and Ta) [18], $Ti_3Si_{0.5}Ge_{0.5}C_2$ [19], Zr_2InC [20], Ti_4AlN_3 [21], Ta_4AlC_3 [22], Ti_3AlCN [23], $Ti_3(Al, Sn_{0.2})C_2$ [23], TiVAlC and TiNbAlC [24], Cr_2GeC and V_2GeC [25]. In all cases, like in Ti_3SiC_2 [26], no phase transitions were observed up to pressures of the order of 55 GPa. K_o of these compounds varied from a high of 261 GPa for Ta_4AlC_3 [22], to a low of 127 GPa for Zr_2InC [20]. For the most part, the relative shrinkage along the c-direction with pressure was greater than

along the *a*-direction; the exceptions were Cr_2AlC, Nb_2AlC [18], and Nb_2AsC [27], where the opposite was true. The Ta-containing phases were unique in that the shrinkages along both directions were quite similar [18,22].

More recently we have shown that replacing C by N in Ti_2AlC results in a decrease in K_o, presumably because of the formation of vacancies on the N and/or Al sites [28]. Replacing Ge by Si in Ti_3GeC_2, on the other hand, does not affect K_o greatly [29]. Replacing Nb by Ti in Nb_2AlC, or V by Ti in V_2AlC, resulted in a decrease in K_o of the solid solution compositions relative to the end members [24].

The combination of easy machinability, relatively low densities (of some of the phases) and high elastic constants, together with the possibility of extremely high damping [16,17] is one that to date had not been possible. Herein we explore the effects of the M-site chemistry on K_o. More specifically, we studied the following phases: Ti_2SnC, Nb_2SnC, Hf_2SnC, Ti_2InC and $(Ti_{0.5}, Zr_{0.5})_2InC$, henceforth referred to as TiZrInC. The results of the In-containing compounds are compared to K_o of Zr_2InC measured previously [20]. Further motivation is our interest in exploring the stability of these phases at high pressures as well as a general understanding of their structure/chemistry/property relationships.

2. Experimental details

The processing details for the M_2SnC (M = Ti, Nb, Hf) compounds can be found elsewhere [30]. In brief, stoichiometric proportions of the Ti, Nb, Hf, Sn and C powders were mixed, cold pressed and sealed in borosilicate glass tubes that were then heated, in a hot isostatic press (HIP), at a rate of 5 °C/min to 850 °C, a temperature at which the glass tubes soften. Upon reaching 850 °C, the HIP was pressurized to 55 MPa and heating was resumed at the same heating rate to the processing temperature, at which point the pressure in the HIP increased to 60–70 MPa. The various compositions were held at the processing temperatures (1250–1325 °C) for different times, varying from 4–24 h [30].

The processing details of the In-containing compounds can also be found elsewhere [31,32]. In brief, stoichiometric proportions of the Ti, Zr, In and C powders were mixed, sealed in borosilicate glass tubes under a mechanical vacuum and heated to 650 °C for 10 h before furnace cooling. This procedure collapsed the tubes and allowed the powders to pre-react. The collapsed tubes were placed in a HIP and heated to 750 °C, at which time the HIP was pressurized to ≈70 MPa before the heating was resumed to a temperature of 1300 °C. Typically the samples were held at temperature for 12 h [31,32].

The X-ray diffraction (XRD) patterns for Ti_2InC, TiZrInC and M_2SnC (M = Ti, Nb) were collected at the high-pressure collaborative access team (HPCAT) beam line at the advanced photon source (Argonne National Laboratory, Chicago, IL). A monochromatic beam – with a wavelength of 0.4066 Å – was focused to a 10 μm spot size on the sample. Diffraction rings were recorded between $2\theta = 1°$ and 35° using an image plate.

For Hf_2SnC, the diffraction patterns were collected using an energy-dispersive mode at the bending magnet beamline of the Cornell High-Energy Synchrotron Source (CHESS). A solid state Ge detector, used to detect the diffracted energy, was calibrated with fluorescence standards of ^{55}Fe and ^{133}Ba, while the $2\theta_o$ of 10° was attuned taking diffraction patterns of a gold standard.

Measurements were conducted at room temperature; powdered samples were pressurized using a gasketed diamond anvil cell (DAC) with a 300 μm culet. A 250 μm initial thickness rhenium gasket was indented to about 50–60 μm.

The stress state of a sample compressed in a DAC can become non-hydrostatic if the material tested is hard and has low compressibility, like the MAX phases. However, it has been shown that the sample pressure can be rendered nearly hydrostatic by using a large volume of a low shear strength material as the pressure-transmitting medium. We have repeatedly shown that Al – with its low shear modulus and lack of phase transitions – was a good pressure-transmitting medium [18–25,28,29,33,34]. Another advantage of Al is the fact that its pressure–volume relationship is well established [35]. In this work, powdered samples were placed between two 15 μm thick Al foils, before packing them in the 100–150 μm hole in the Re gasket. More details can be found in any of our previous papers [18–25,28,29].

The FIT2D software [36,37] was employed to convert the image plate records into 2θ's and intensities. The *a* and *c* lattice cell parameters were determined using least squares refinement on individually fitted peaks.

The bulk moduli were computed using ab initio density functional calculations, conducted using the Vienna Ab initio Simulation Package (VASP) [38] with the MedeA [39] interface. All calculations were carried out using the projector augmented wave (PAW) [40,41] and the generalized gradient approximation (GGA) [42]. Relaxed structures were calculated and energies were converged with respect to the *k*-mesh using MedeA's convergence method. Subsequent calculations were carried out using the *k*-mesh resulting from the convergence. The bulk moduli were calculated using the method outlined in Ref. [43], which in summary consisted of calculating the volume of the relaxed unit cell and then calculating the energy of the unit cell relaxed with the additional condition that the volume be fixed. The relationship between the energy and the volume was then used to determine the bulk moduli using the Birch–Murnaghan equation [44,45].

3. Results

The XRD spectra and their pressure dependences are shown in Fig. 1a–f. The space group adopted for all phases is $P6_3/mmc$, and the lattice parameters obtained (Table 1) are in good agreement with previous work.

Fig. 2 plots the variations in relative unit cell volumes, V/V_o, as a function of applied quasi-hydrostatic pressure P. V_o is volume of unit cell when $P = 1$ atm. Second-order polynomial least square fits of these data resulted in the coefficients listed in Table 2. Fitting the same results to the Birch–Murnaghan equation [45]

$$P = 3/2K_o[(V/V_o)^{-7/3} - (V/V_o)^{-5/3}]$$
$$\times [1 + 3/4(K_o' - 4)[(V/V_o)^{-2/3} - 1]]$$

yields K_o values of 148 ± 3 GPa for Ti_2InC and 131 ± 3 GPa for TiZrInC. For the M_2SnC compounds, K_o was 152 ± 3 GPa for Ti_2SnC, 169 ± 4 GPa for Hf_2SnC and 180 ± 5 GPa for Nb_2SnC. It follows, not surprisingly, that the K_o values reported herein are in line with previous MAX phase results in that these solids are elastically quite stiff.

Fig. 3 plots the relative changes in lattice parameters, a/a_o and c/c_o, as a function of P. The subscripts refer to the values of *a* and *c* when $P = 1$ atm. Note that for all compositions the contraction along the *c*-direction is greater than that along the *a*-direction. Second-order polynomial least square fits of these data resulted in the coefficients listed in Table 3.

4. Discussion

The lattice parameters reported herein are in good agreement with previous work (Table 1). When these, and related lattice parameters, are plotted versus the atomic radii, r_M, of the *M* elements (Fig. 4) a somewhat complicated picture emerges. (In Fig. 4, r_M for the solid solutions was taken to be the average of the end members' radii. Also, the *y*-axis scales were chosen
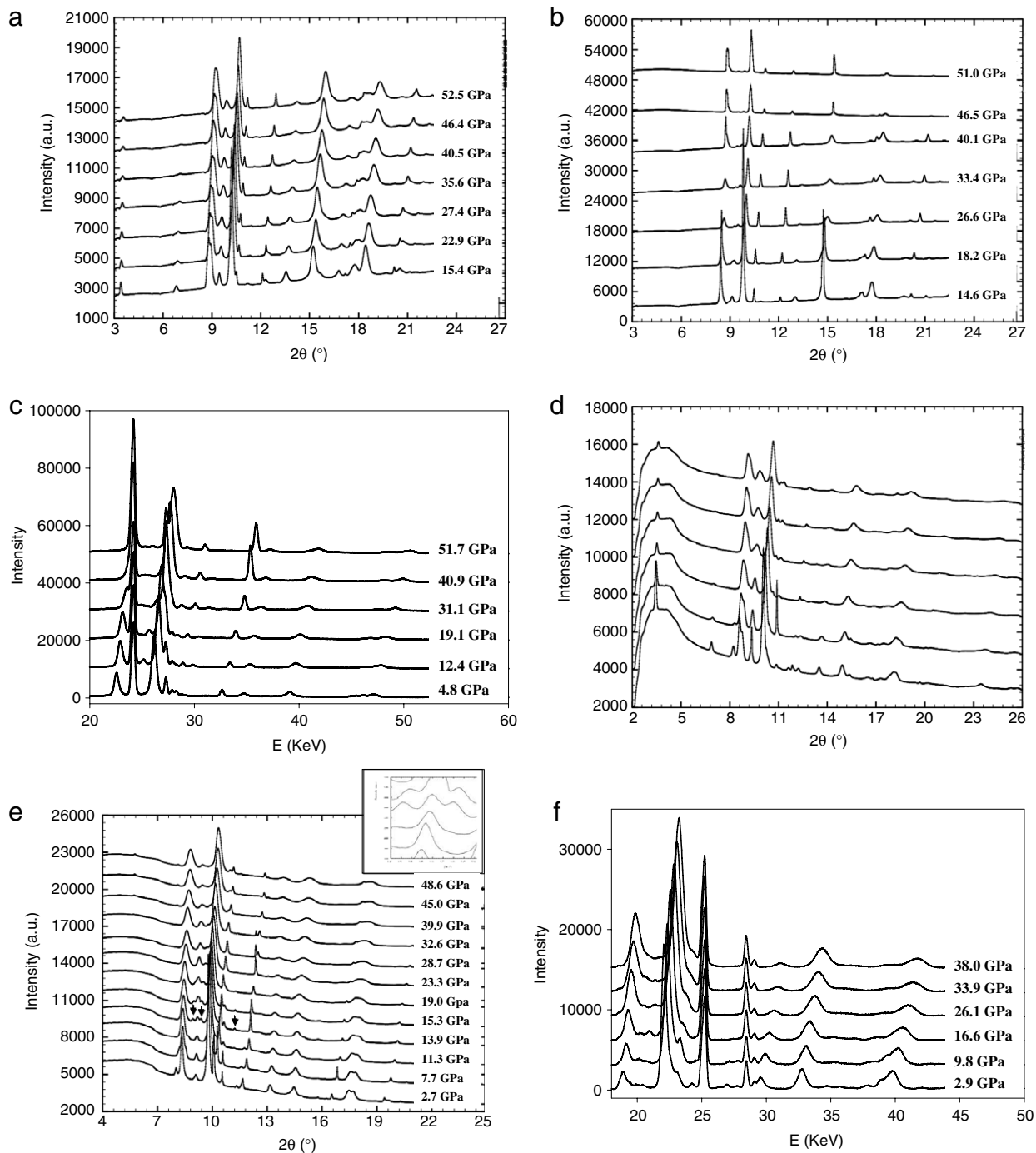
Fig. 1. Functional dependence of high-pressure XRD spectra for (a) Ti_2InC, (b) TiZrInC, (c) Zr_2InC, (d) Ti_2SnC, (e) Nb_2SnC and (f) Hf_2SnC on quasi-hydrostatic pressure, *P*. Upon compression, most peaks remain visible until the highest pressures reached. With increasing *P*, the peaks become broader, lose intensity, and some merge together. In Fig. 1e the arrows point to extra reflections that do not belong to Nb_2SnC; the inset show the additional reflections.

to reflect the same percentage change in the lattice parameters.) To make sense of the results, we focus first on the In series (Fig. 4a). Here two sets of lines emanate from the Ti_2InC corner, one joining Hf_2InC, and the other, at a steeper slope, joining Hf_2InC. Not surprisingly, the TiHfInC lattice parameters follow Vegard's law, i.e. they fall on the Ti–Hf line. Interestingly, but consistent with our ab initio calculations (Table 1), the lattice parameters of the Hf-containing compounds are lower than those for the Zr-containing ones, despite the fact that the radius of Hf is larger than that of Zr. The Nb_2InC results are intriguing, however. The *a*-lattice parameter (red symbols, left *y*-axis) fall on the Ti–Hf line; the *c*-

lattice parameter (black symbols, right *y*-axis) on the Ti–Zr line. The identical behavior is seen for Nb_2SnC in the M_2SnC system (Fig. 4b).

The situation for the Sn-containing compounds is similar; the lines joining the respective parameters of Ti_2SnC to Zr_2SnC are steeper than the ones joining Ti_2SnC to Hf_2SnC. The lattice parameters of Zr_2SnC ($a = 3.358$ Å and $c = 14.57$ Å) were taken from Ref. [30].

For the most part, most peaks remain visible until the highest pressures reached (Fig. 1). With increasing pressure, the peaks become broader, lose intensity, and some merge together. Except for Nb_2SnC, no extra peaks appear in the patterns up to ≈50 GPa, a